STM JOURNALS

Investigation of DC link Capacitor Failures in DFIG based Wind Energy Conversion System

Ali M. Eltamaly and Ammar Anwar Khan*
King Saud University, Riyadh, Saudi Arabia

ABSTRACT

This paper presents the effects of DC link electrolytic capacitor failure of DFIG based wind energy conversion system (WECS). The degradation of electrolytic capacitor can lead to the failure of DC link. As DFIG based WECS utilize low power converter, so there is a need to explore the effects of capacitor failure. This failure (short circuit of capacitor or open circuit) leads to the power outages, high machine currents, high transient currents in rotor circuit, low terminal voltage of the generator and increase in generator speed. For this purpose aggregated model of DFIG is implemented in the MATLAB/ Simulink to study the effects of DC link capacitor short/open circuit on different parameters of system.

Keywords: *DFIG, DC link failure, capacitor short circuit, stator flux orientation, capacitor open circuit*

****Author for Correspondence*** E-mail: eltamaly@ksu.edu.sa Mob: +966553334130

INTRODUCTION

DFIG proves itself as one of the successful generator topologies for wind energy conversion systems due to its variable speed operation and low power rating three phase AC/DC/AC converter. AC/DC/AC PWM converters are widely used in motor drives, wind power generation [1], unified power quality conditioners [2] etc. These converters usually consist of DC link of array of electrolytic capacitors as energy buffer. Electrolytic capacitors are preferred due to their large capacitance per volume and low cost per capacitance. However they are sensitive to temperature, frequency and have low reliability [3-4]. The lifetime of electrolytic capacitor is usually shorter than the other components of the converter. Reference [1] reported that 72% of the power supplies failures were due to electrolytic capacitor failures. The capacitors are considered to be over when, with the passage of time, their capacitance is decreased by more than 25% [5]. It has been reported in many researches that electrolytic capacitors are the weakest link in power electronic converters [7-12]. The failure of DC link electrolytic capacitor can lead to either short circuit or open circuit of DC link while remaining the converters intact. The capacitor degradation is due to the effects of thermal, electrical, mechanical and environmental stresses and there can be any reason of its failure. The primary failure mechanism is the evaporation of electrolytic solution and its loss through end seal. Temperature rise accelerates the evaporation rate. This evaporation leads to the decrease in capacitance and increase in ESR (equivalent series resistance) which increases the losses. Thus the degradation process continues till the capacitor fails. Other modes of failures are mentioned as [7]:

1. Rupturing or explosion of capacitor due to excessive internal pressure (when normal operating ranges are exceeded).
2. Open/short circuit failures due to repeated mechanical stress on the leads or capacitor.
3. Corrosion of leads due to cleaner, adhesive, coating material (mainly for PCB mounted capacitors), or other foreign material.

Despite the importance of electrolytic capacitors, the related research is very limited in the field of switch mode power supplies, drives and wind energy conversion systems. There a need to study the effects of failure of DC link electrolytic capacitor and also to estimate the remaining life or degree of degradation of capacitor. One of the common methods to estimate the life of capacitor is monitoring the ESR as reported in [10]. As the DC linked capacitor converters are installed inside the systems, so they make it difficult to detach the component and measure the degradation of the capacitor. Also it is very difficult to monitor manually of off-shore or on-shore wind turbines having high towers. References [13] and [14] explored the capacitance and online condition monitoring of the electrolytic capacitors. This paper deals with the study of results of DC link electrolytic capacitor failure on the DFIG system. High and comparatively low power converters are widely used in DFIG, permanent magnet synchronous generator or induction generator based wind energy conversion systems. A 9MW wind farm is aggregated modeled in MATLAB/Simulink to study the effect of lumped model of DC link electrolytic capacitor failure. The next sections discuss in details about the modeling, control, effects of DC link failure and simulation results.

Wind Energy System Model

Wind energy system consists of wind turbine that is connected to synchronous or asynchronous generator which generates the power to feed the grid. In case of doubly fed induction generator, it has a low power converter in its rotor side circuit to control the slip speed. Figure 1 shows the general representation of a DFIG based wind farm.

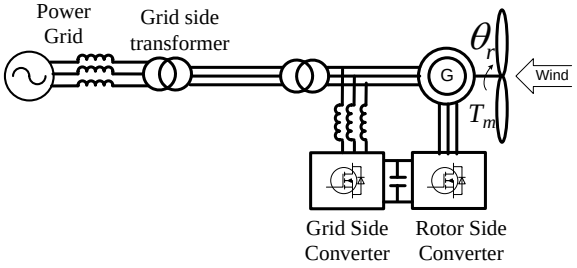

Fig. 1 Schematic of Interconnection of DFIG with Electric Utility.

Aerodynamic Model of Wind Turbine

The power exploited by wind turbine from the wind is given by [15]:

$$P_m = \frac{1}{2} C_p \rho \pi R^2 u^3 \qquad (1)$$

It means that as wind speed changes, the pitch angle or tip speed ratio is so adjusted to utilize maximum power contained in wind. The tip speed ratio is the ratio between the tip speeds $R\Omega$ to the wind speed u. This tip speed ratio λ is defined as [15]:

$$\lambda = \frac{R\Omega}{u} \qquad (2)$$

The power coefficient C_p is the function of tip speed ratio λ and the pitch angle β and it given by [16]:

$$C_p(\lambda,\beta) = c_1(\frac{c_2}{\lambda_i} - c_3\beta - c_4)e^{-\frac{c_5}{\lambda i}} + c_6\lambda \quad (3)$$

And λ_i is given as:

$$\frac{1}{\lambda_i} = \frac{1}{\lambda + c_7\beta} - \frac{c_8}{\beta^3 + 1} \quad (4)$$

The coefficients from c_1 to c_8 are defined as in Ref. [16].

Modeling of DFIG

A fifth-order state space model of DFIG and second order drive train model is given below [17]. All electrical variables and parameters are referred to the stator. This is indicated by the subscripts in the machine equations given below. The subscripts used are defined as follows:

d : d-axis quantities

q : q- axis quantities

r : rotor quantities

s : stator quantities

l : leakage inductance quantities

$$v_{qs} = R_s i_{qs} + \frac{d}{dt}\phi_{qs} - \omega_e\phi_{ds} \quad (5)$$

$$v_{ds} = R_s i_{ds} + \frac{d}{dt}\phi_{ds} - \omega_e\phi_{qs} \quad (6)$$

$$v_{qr} = R_r i_{qr} + \frac{d}{dt}\phi_{qr} - (\omega_e - \omega_r)\phi_{dr} \quad (7)$$

$$v_{dr} = R_r i_{dr} + \frac{d}{dt}\phi_{dr} - (\omega_e - \omega_r)\phi_{qr} \quad (8)$$

$$T_e = \frac{3}{2}P(\phi_{ds}i_{qs} - \phi_{qs}i_{ds}) \quad (9)$$

The fluxes are given as:

$$\phi_{qs} = L_s i_{qs} + L_m i_{qr} \quad (10)$$

$$\phi_{ds} = L_s i_{ds} + L_m i_{dr} \quad (11)$$

$$\phi_{qr} = L_r i_{qr} + L_m i_{qs} \quad (12)$$

$$\phi_{dr} = L_r i_{dr} + L_m i_{ds} \quad (13)$$

$$L_s = L_{ls} + L_m \quad (14)$$

$$L_r = L_{lr} + L_m \quad (15)$$

$$\frac{d}{dt}\theta_m = \Omega \quad (16)$$

$$\frac{d}{dt}\Omega = \frac{1}{2H}(T_e - F\Omega - T_m) \quad (17)$$

The stator active power can be defined as [19];

$$P_s = \frac{3}{2}(v_{ds}i_{ds} - v_{qs}i_{qs}) \quad (18)$$

The stator reactive power as:

$$Q_s = \frac{3}{2}(v_{qs}i_{ds} - v_{ds}i_{qs}) \quad (19)$$

And electrical angle is:

$$\theta_e = \int \omega_e dt = \tan^{-1}\frac{v_\beta}{v_\alpha}$$

Rotor-Side Converter Control

By aligning the d-axis of the reference frame (stator flux orientation) along with the grid voltage position $v_{qs}=0$ and $v_{ds}=V_s$ the active and reactive power can be obtained by using (18) and (19):

$$P_s = \frac{3}{2}(v_{ds}i_{ds}) \quad (20)$$

$$Q_s = \frac{3}{2}(-v_{ds}i_{qs}) \quad (21)$$

And i_{qs} can be obtained as:

$$i_{qs} = -\frac{i_{qr}L_m}{L_s} \quad (22)$$

Using (22) in (21):

$$Q_s = \frac{3L_m}{2L_s}(v_{ds} i_{qr}) \quad (23)$$

From (23) it can be noticed that the stator reactive power Q_s can be controlled by the q-axis rotor current i_{qr}. The reference for the torque can be obtained from:

$$T_e = \frac{L_m}{L_s}(\phi_{qs} i_{dr} - \phi_{ds} i_{qr}) \quad (24)$$

By using stator flux orientation control and assuming ϕ_{ds}=0:

$$T_e = \frac{L_m}{L_s}(\phi_{qs} i_{dr}) \quad (25)$$

The value of ϕ_{qs} can be obtained from (6) as:

$$\phi_{qs} = \frac{v_{ds} - R_s i_{ds}}{-\omega_e} \quad (26)$$

Equations (23) and (25) give the references for i_{qr} and i_{dr} respectively to independently control active and reactive power of the stator.

Grid-Side Converter Control

The main function of the GSC is to control the DC link voltage and to control active and reactive power from the DC link to the gird through grid side converter. If the dc voltage, V_{dc} is greater than its reference value V_{dc}^* this means that more power must be moved from the DC link to electric utility via grid-side converter. The DC link voltage is controlled by using stator voltage orientation control [19]. This scheme permits independent control of the DC link voltage and reactive power. The active and reactive power from the GSC to electric utility is obtained from the following:

$$P_{gc} = \frac{3}{2}(v_{ds} i_{dgc} + v_{qs} i_{qgc}) \quad (27)$$

$$Q_{gc} = \frac{3}{2}(v_{qs} i_{dgc} - v_{ds} i_{qgc}) \quad (28)$$

Substituting for V_{qs} in (27) and (28):

$$P_{gc} = \frac{3}{2}(v_{ds} i_{dgc}) \quad (29)$$

$$Q_{gc} = \frac{3}{2}(-v_{ds} i_{qgc}) \quad (30)$$

It is clear from these two equations that the active and reactive powers can be controlled independently by using the reference currents from (29) and (30). The decoupled control is implemented in order to control the active and reactive power by rotor and grid side converters. The reference values of voltages obtained from reference values of currents are fed to the PWM controllers to generate the required signals to operate the converters.

DC Link Capacitor Failure

Off-shore or on-shore wind turbines bear harsh environmental conditions. The incor--poration of array of electrolytic capacitors in DC link of converter makes it vulnerable to periodic degradation. This degradation of capacitor over the passage of years or loose link may result in short circuit or open circuit of capacitor in the DC link. If the capacitor is short circuited it will make the DC voltage as zero in the rotor and grid side converter controllers. These controllers depend on V_{dc} for determining the

modulation index for active power, reactive power and DC link voltage control. In case of DC link short circuit, the GSC will try to charge the capacitor in order to raise the voltage of capacitor; hence it will exchange more power from the grid. On the other hand, the firing sequences of the switches are also dependent upon the DC link voltage. The modulation indices of rotor side convertor and grid side convertors are determined by taking into account the DC link voltage. Equation (31) gives the relation that is used for determining the modulation indices of RSC and GSC.

$$m = Vnom * 2 * \frac{\sqrt{\frac{2}{3}}}{V_{dc}} \qquad (31)$$

The DC voltage is present in the denominator of the equation and can present the divide by zero error if the measured DC voltage by the sensors is 0V. However, based upon above equation, the converters will try to achieve maximum modulation indices. Same is the case with open circuit capacitor link. This will create the fluctuating DC link voltage in which grid side converter will try to stable the DC link voltage and rotor side converter will try to generate the sequence for controlling the torque. Either of these problems leads to the machine instability and machine suffers from power outages, low terminal voltage, high currents (in case of DC link short circuit) and high rotor speed. Next section deals with the simulation of both the cases and their results on machine output parameters.

SIMULATION RESULTS

A 9MW aggregated model of DFIG based wind farm is simulated in Simulink. The simulation time 0.4s and DC link failures of short circuit or open circuit occur at 0.2s. The model starts simulation using steady state values. Table I and Table II give the pre-fault and during fault (short circuit and open circuit) parameters of wind farm. The whole wind farm is simulated as a single block and only the effect of lumped DC link short circuit capacitor is studied to see the effects of this failure on the same system. Grid is modeled as 2500MVA short circuit capacity with $X_0/X_1=3$. The generator generates at voltage level 575V which is stepped up to 25kV and transmitted to the connection point through 30km transmission line and finally connected to the grid by a step up transformer 25kV/132kV. Simulation is performed by using ode45 in Simulink with step size of 1 microsecond. Figure 2 to Figure 9 show the behavior of generator output parameters during the short circuit of capacitor. For simulation purposes, the short circuit is applied by simply by passing the capacitor with a zero resistance link.

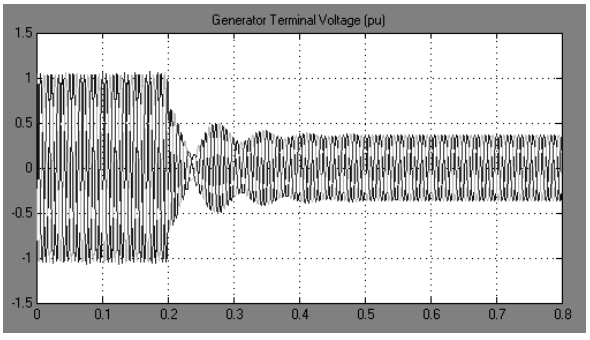

Fig. 2 Generator Terminal Voltage During Short Circuit of Capacitor.

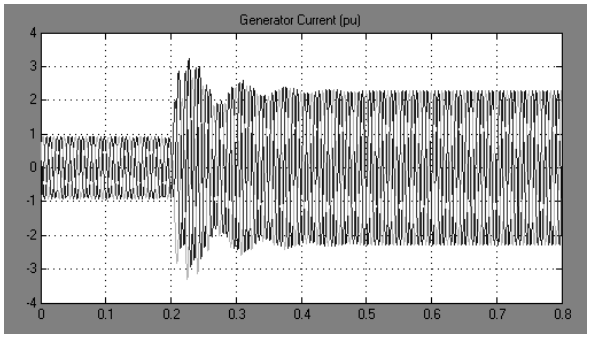

Fig. 3 Generator Complete Current During Short Circuit of Capacitor.

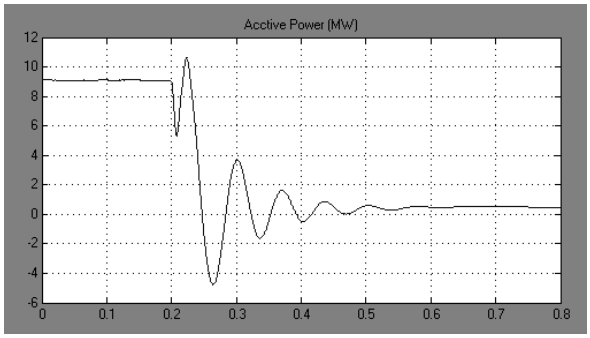

Fig. 4 Generator Active Power during Short Circuit of Capacitor.

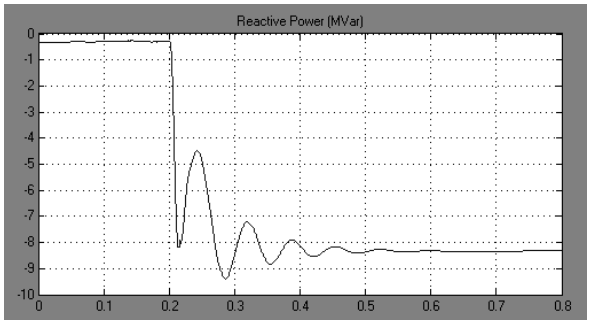

Fig. 5 Generator Reactive Power During Short Circuit of Capacitor.

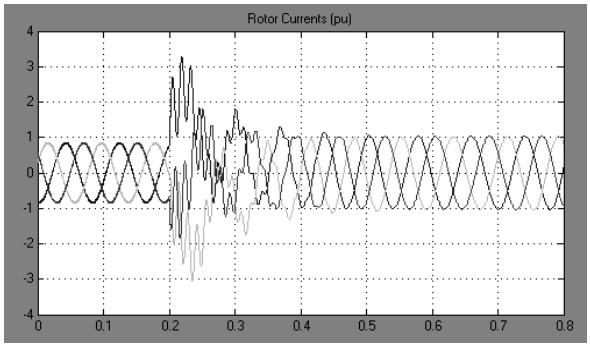

Fig. 6 Generator Rotor Currents During Short Circuit of Capacitor.

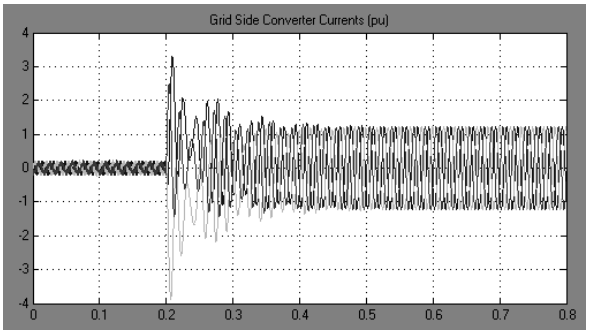

Fig. 7 Grid Side Converter Currents during Short Circuit of Capacitor.

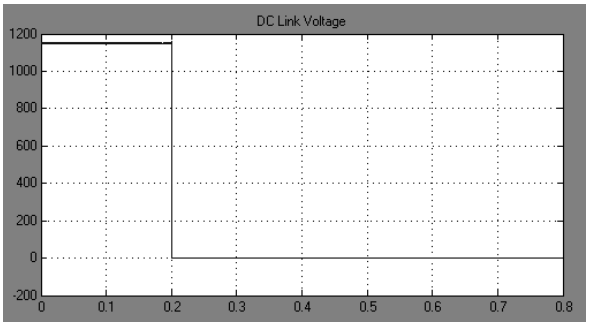

Fig. 8 DC Link Voltage During Short Circuit of Capacitor.

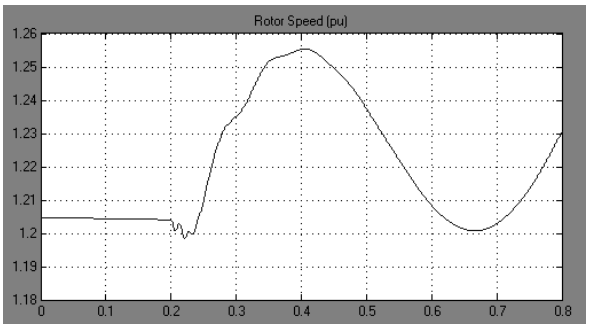

Fig. 9 Rotor Speed during Short Circuit of Capacitor.

Figure 2 shows the generator terminal voltage. The simulation was run with steady state and at t=0.2s, short circuit was applied. The voltage of the generator reached to 0.4pu of its original value. The generator currents reached up to 2pu with the transient peak reaching 3pu as shown in Figure 3. The increased generator currents will result in increased rotor currents. The rotor currents reached up to 1 pu (previously 0.8 pu) with the transient peak touching 3pu as seen in

Figure 6. The grid side converter will try to increase the DC link voltage and will result in higher currents as shown in Figure 7. Figure 4 and Figure 5 show the generator active and reactive powers. After the DC link capacitor short circuit, the generator loses its active power generation and terminal voltage. However the demand for reactive power is increased. This is due to the disturbance in the control of grid side converter. Figure 9 shows the rotor speed. The rotor speed fluctuates around its rated speed during the short circuiting of capacitor.

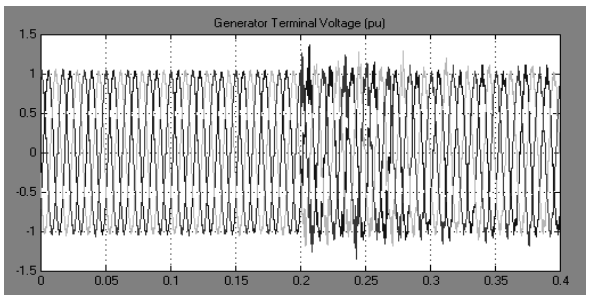

Fig. 10 Generator Terminal Voltage During Open Circuit of Capacitor.

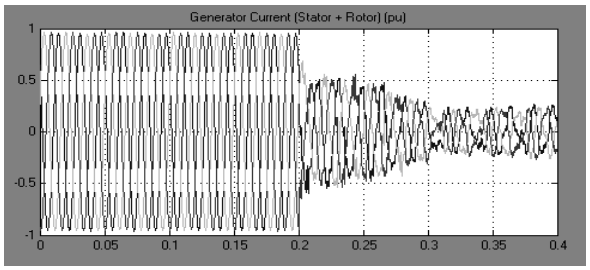

Fig. 11 Generator Complete Currents During Open Circuit of Capacitor.

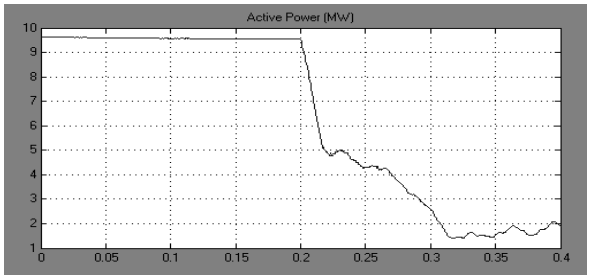

Fig. 12 Generator Active Power During Open Circuit of Capacitor.

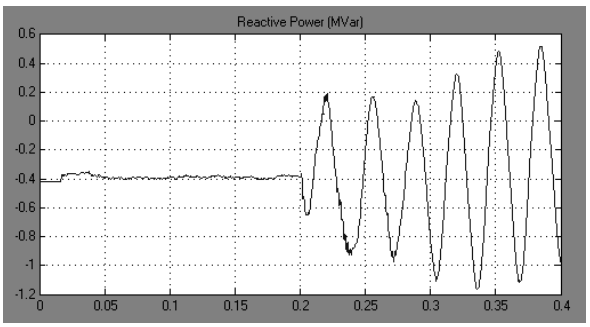

Fig. 13 Generator Reactive Power during Open Circuit Of Capacitor.

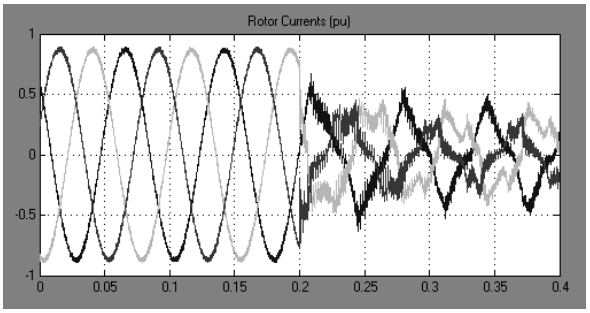

Fig. 14 Rotors Currents during Open Circuit of Capacitor.

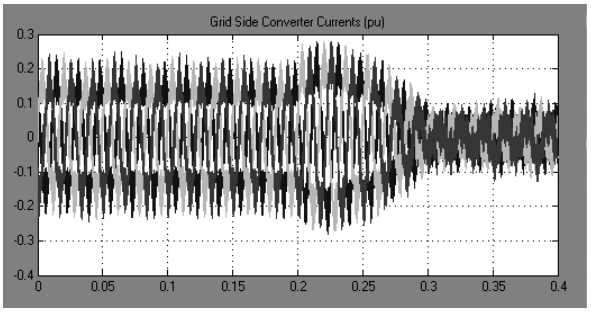

Fig. 15 Grid Side Converter Currents During Open Circuit of Capacitor.

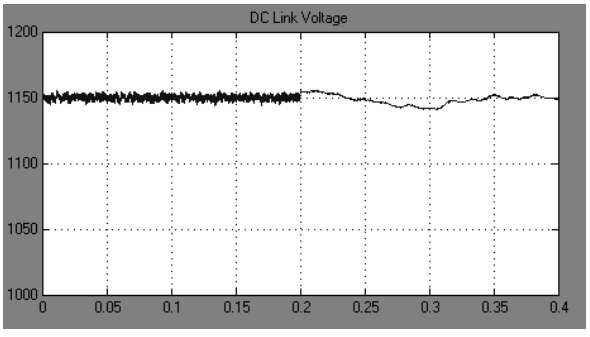

Fig. 16 DC Link Voltage During Open Circuit of Capacitor.

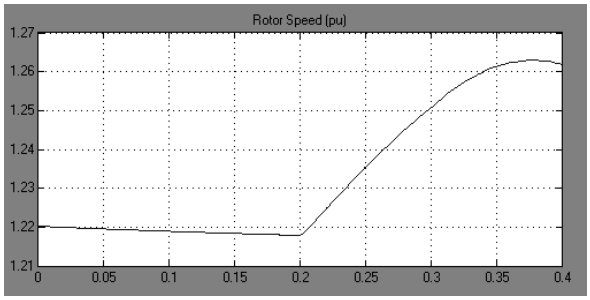

Fig. 17 Rotor Speed During Open Circuit of Capacitor.

Figure 10 to Figure 17 show the generator characteristics during open circuiting of the DC link electrolytic capacitor. Figure 10 shows that after the DC link capacitor failure, the generator terminal voltage remained 1pu but it was distorted as seen in figure. The generator current control was lost and generator currents reached up to 0.2 pu as shown in Figure 11. The generator lost its active power generation capability as given in Figure 12. Figure 13 shows the reactive power of the generator. Due to oscillating DC link voltage the reactive power oscillated around 0MVar as desired reactive power is 0MVar. Figure 14 and Figure 15 show the rotor and grid side converter currents. Both dropped up to 0.5pu and 0.1pu respectively. Figure 16 shows the DC link voltage which fluctuates during the fault. Figure 17 shows the rotor increased speed above the rated speed.

From Figure 2 to Figure 17, it is seen that DC link capacitor failure leads to power loss and low generator terminal voltage, high rotor speed and failure of rotor side and grid side converters control. The effects of failure conditions are serious when this generator is considered to be a part of wind farm. Low terminal voltage, high currents, loss of active power and reactive power fluctuation can bring disturbance to the complete system. As DC link is represented by a lumped capacitor in the simulation. In reality, arrays of capacitors are used. However, due to aging and deterioration due to long time of service, they can suffer from either short circuit or open circuit problem.

Table I. States of the Parameters at Pre-Fault and during Fault (short circuit capacitor).

Parameters	**Pre-fault states**	**During fault**
Active power	9MW	0MW
Reactive Power	0MVar	-8MVar
Generator terminal voltage	1pu	0.4pu
Generator current	1pu	2.1pu
Rotor current	0.8pu	2pu
DC link voltage	1150V	1150V
Grid side converter current	0.3pu	1.2pu
Rotor speed	1.20pu	1.25

Table II. States of the Parameters at Pre-Fault and During Fault (Open Circuit Capacitor).

Parameters	Pre-fault states	During fault
Active power	9MW	2MW
Reactive Power	0MVar	Oscillates around 0MVar
Generator terminal voltage	1pu	1pu but distorted
Generator current	1pu	0.25pu
Rotor current	0.8pu	0.5pu
DC link votlage	1150V	Oscillates around 1150V
Grid side converter current	0.3pu	0.1pu
Rotor speed	1.20pu	1.26

CONCLUSIONS

The behavior of DC link short and open circuit is simulated in Simulink to observe the output parameters of DFIG based wind energy conversion system. DC link of DFIG constitutes the array of electrolytic capacitors. Electrolytic capacitors degrade with the passage of long time. DC link represents the weakest link in converter and is vulnerable to either short circuit or open circuit. During the short circuiting of capacitor, the generator terminal voltage falls, its active power capability is lost with high rotor and stator currents. The grid side converter exchanges high currents than the nominal values. In open circuit condition, the active power capability is lost and currents controllers at RSC and GSC fail. Rotor speed increases in both conditions. These conditions are serious for other wind turbines in the same wind farm. The disturbance in one generator can make complete wind farm unstable. However there is a need to study the behavior of single generator DC link failure on other generators performance in the wind farm.

REFERENCES

1. Pena R., Clare J. & Asher G. M. *IEE Proceedings Electric Power Applications* 1996. 143(3) 231–241p.
2. Fujita H. & Akagi H. *IEEE Transactions on Power Electronics* 1998. 13(2) 315–322p.
3. Military Handbook 217 F. Feb. 28, 1995.
4. Matsushita Electronic Components Co. Mar. 2, 2000.
5. Hitachi AIC Inc. Tokyo, Japan. 1999.
6. Harada K., Katsuki A. & Fujiwara M. *IEEE Transactions on Power Electronics* Oct., 1993. 8(4) 355–361p.
7. Lee K.W., Kim M., Yoon J. et al. *IEEE Transactions on Industrial Applications*, pp. 1606–1613, Sept. /Oct. 2008.
8. Gasperi M. L. *IEEE Transactions on Industry Applications* Nov./Dec. 2005. 41(6) 1430–1435p.
9. Sankaran V. A., Rees F. L. & Avant C. S. *Proceedings of IEEE IAS Annual Meeting* Oct. 1997. 1058–1065p.
10. Layhani A., Venet P., Grellet G. et al. *IEEE Transactions on Power Electronics* Nov. 1998. 13(6) 1199–1207p.

11. Ondel O., Boutleux E. & Venet P. *Proceedings of IEEE PESC* June, 2004. 4360–4364P.
12. Venet P., Perisse F., El-Husseini M. H. et al *IEEE Industry Applications Magazine* Jan–Feb., 2002. 8(1). 16–20p.
13. Michael L. Gasperi *IEEE Industry Applications Society Annual Meeting* New Orleans, Louisiana. Oct. 5–9, 1997.
14. Lee D.C., Lee K. J., Seok J. K. et al. *IEE Proceedings Electric Power Applications* Nov., 2005. 152(6) 1503–1508p.
15. Ali M. Eltamaly Journal of King Saud University. Engineering Sciences. 2007. 19(2) 223–228p.
16. Heier S., John Wiley & Sons Ltd, 2nd Edition. ISBN 0470868996. 2006.
17. Krause P. C., Wasynczuk O. & Sudhoff S. D., "*Analysis of Electric Machinery",* book, IEEE Press. 2002.
18. Vas P. *Oxford science Publications*. ISBN 13: 9780198564652. 1998.
19. Yao J., Li H., Liao Y. et al. *IEEE Transactions on Power Electronics* 2008. 23(3) 1205–1213p.

APPENDIX

Nomenclature

P_m	Mechanical power from wind turbine
ρ	Air density (kg/m^3)
R	Radius of the swept area by the blades (m)
u	Velocity of the wind (m/sec)
C_p	Power coefficient.
Ω	Angular velocity of the shaft (rad/sec)
λ	Tip speed ratio
β	Blades pitch angle
λ_{nom}	Tip speed ratio associated with the maximum coefficient of performance
R_s ,L_{ls}	Stator resistance and leakage inductance
R_r,L_{lr}	Rotor resistance and leakage inductance
L_m	Magnetizing inductance
L_s , L_r	Total stator and rotor inductances
v_{qs} , i_{qs}	q axis stator voltage and current
v_{qr} , i_{qr}	q axis rotor voltage and current
v_{ds} , i_{ds}	d axis stator voltage and current
v_{qr} , i_{qr}	d axis rotor voltage and current
ϕ_{qs} , ϕ_{ds}	Stator q and d axis fluxes
ϕ_{qr} , ϕ_{dr}	Rotor q and d axis fluxes
ω_r	Angular velocity of the rotor
θ_m	Rotor angular position
P	Number of pole pairs
ω_e	Electrical angular velocity ($\Omega * P$)
Θ_e	Electrical rotor angular position ($\theta_m * P$)
T_e	Electromagnetic torque
T_m	Shaft mechanical torque
J	Combined rotor and load inertia coefficient. Set to infinite to simulate locked rotor
H	Combined rotor and load inertia constant. Set to infinite to simulate locked rotor
F	Rotor and load viscous friction coefficient
P_s, Q_s	Stator active and reactive power
P_{gc} , Q_{gc}	Active and reactive power from the GSC to electric utility.
i_{dgc} , i_{qgc}	d and q-axes of current from GSC.
V_{dc}	DC-link voltage